INSTITUTE OF PHYSICS PUBLISHING JOURNAL OF OPTICS A: PURE AND APPLIED OPTICS
J. Opt. A: Pure Appl. Opt. **4** (2002) S168–S174 PII: S1464-4258(02)32972-6

Characterization of rough self-affine surfaces by electromagnetic wave scattering

Ingve Simonsen[1,2], Annie Tarrats[3] and Damien Vandembroucq[4]

[1] Nordisk Institut for Teoretisk Fysik–Nordita, Blegdamsvej 17, DK-2100 Copenhagen, Denmark
[2] Department of Physics, The Norwegian University of Science and Technology, N-7491 Trondheim, Norway
[3] Laboratoire d'Energétique Moléculaire et Macroscopique, Combustion CNRS, Ecole Centrale Paris, 92295 Châtenay-Malabry Cedex, France
[4] Unité Mixte CNRS/Saint-Gobain 'Surface du Verre et Interfaces', 93303 Aubervilliers Cedex, France

Received 23 January 2002
Published 14 August 2002
Online at stacks.iop.org/JOptA/4/S168

Abstract
We study the scattering of electromagnetic waves from metallic self-affine surfaces, and review earlier approximative results for the angular distribution of the scattered light (the mean differential reflection coefficient). Furthermore, experimental scattering data for industrial cold-rolled aluminium surfaces that show self-affine scaling invariance are presented. Comparison between these experimental data and approximative analytic and rigorous numerical simulation results shows very good agreement over the dominating angular interval where most of the scattered power is distributed. The excellent quality of this agreement suggests that light scattering can be used as a cheap, robust and versatile (inverse scattering) tool for characterizing self-affine metallic surfaces, i.e. used to estimate roughness exponents as well as topothesies and the related slope parameters.

Keywords: Wave scattering, self-affine, fractal, aluminium, inverse problems

1. Introduction

Wave scattering from self-affine fractal surfaces has been studied intensively for the last 20 years. In the mid-1980s theoretical results were given by Jakeman *et al* [1, 2] and Sinha *et al* [3] for the angular distribution of the scattered light. These results were later extended and applied to the experimental characterization of thin-film growth. Consult, for example, the recent review by Zhao *et al* [4] for details. More recently, direct rigorous numerical calculations have been performed for electromagnetic wave scattering from one-dimensional self-affine surfaces [5–8] and the results of such calculations have successfully been compared with analytic expressions that can be derived from a Kirchhoff approximation [9, 10]. However, none of these studies compared analytic and simulation results with experimentally obtained scattering data. This will therefore be the main goal of the present paper.

In the following we first recall the definition of self-affine surfaces and the parameters which allow us to characterize them. We then give the expression for the angular dependence of the scattered light in the Kirchhoff approximation in the case of s polarization of the incident light and focus on the incoherent scattering peak. We show evidence that this peak is slightly shifted away from the specular angular position. We finally show experimental results obtained for cold-rolled aluminium surfaces and compare them with both the Kirchhoff solution and rigorous numerical simulation results.

2. Characterization of rough self-affine surfaces

A large number of real surfaces can be described through a fractal formalism. This is, for example, the case for fracture surfaces [11] or deposition surfaces [12] to mention a few. However, industrial processes may also lead to the formation

of self-affine surfaces. To illustrate this, in figure 1 we show an atomic force microscopy (AFM) image of a thin aluminium plate produced by cold rolling. This result has been obtained by Boehm and Plouraboué [13], who showed that such a surface shows a self-affine scaling over three orders of magnitude ranging in scale from 50 nm up to 50 μm.

Although widely used for more than 20 years, the characterization of rough surfaces by scale-invariant, fractal or self-affine tools sometimes suffers from ambiguous definitions. This is especially the case for the concept of *fractal dimension*, which is commonly used in practice although poorly defined in the case of surfaces. Below we summarize the main parameters used to characterize a rough surface when a scaling-invariant description is relevant.

Let us start by considering the statistical description of surface roughness, that for simplicity is assumed to be planar on average. A two-dimensional coordinate system is arranged so that the x-axis coincides with the mean planar surface, and the z-axis is directed upward into the (assumed) vacuum above the metal surface. Furthermore, it will be assumed that the height fluctuations can be quantified by a single-valued real function $z = h(x)$. The height statistics is described by the height distribution function and the height–height correlation function. In the case of short-range correlations, the roughness can thus be characterized by two quantitative parameters—the standard deviation of heights and the correlation length, i.e. the lateral distance over which the correlation function drops to $1/\mathrm{e}$ of its initial value. Let us now turn our attention to the case of scale invariance. From a mathematical point of view the roughness is said to be scale invariant if it remains statistically invariant under anisotropic transformations of the form

$$\Delta x \to \lambda \Delta x \qquad \Delta z \to \lambda^{\zeta} \Delta z. \tag{1}$$

Here, Δz corresponds to the height difference between two points separated by a (lateral) distance Δx. The Hurst exponent ζ (also known as the roughness exponent) is a constant parameter that characterizes the invariance. Finally the multiplicative factor λ can take on any real positive value. Let $\mathcal{P}(\Delta z, \Delta x)$ denote the probability distribution of height increment Δz for a given horizontal separation Δx. Hence, the statistical scale invariance, given by equation (1), implies

$$\mathcal{P}(\Delta z, \Delta x)\mathrm{d}(\Delta z) = \mathcal{P}(\lambda^{\zeta} \Delta z, \lambda \Delta x)\mathrm{d}(\lambda^{\zeta} \Delta z) \tag{2a}$$

which has the consequence that

$$\mathcal{P}(\Delta z, \Delta x) = \frac{1}{\Delta x^{\zeta}} \phi\left(\frac{\Delta z}{\Delta x^{\zeta}}\right) \tag{2b}$$

where ϕ is some continuous function.

This property has a simple and direct consequence: a roughness measurement depends on the lateral extension over which it is performed. For example the standard deviation or root mean square (RMS) of the height differences, $\sigma(\Delta x)$, depends on the distance, Δx, according to

$$\sigma(\Delta x) \propto \Delta x^{\zeta}. \tag{3}$$

Surfaces obeying this type of anisotropic scale invariance are said to be *self-affine* and they are characterized by the roughness (or Hurst) exponent ζ. However, the roughness cannot be characterized *only* by this parameter. In particular, this roughness exponent gives no information about the amplitude of the height fluctuations. For any given spatial separation, this amplitude can be very small or very large independent of ζ. Hence, we need an additional parameter to characterize the amplitude of these height fluctuations. The definition of such a parameter is less simple than it could appear at first glance and may be dependent on the physical system studied. A simple geometrical choice is to specify the typical roughness, $\sigma(\ell_0)$, obtained at a reference scale, ℓ_0 (the wavelength for example), and we have directly from equation (3)

$$\sigma(\Delta x) = \sigma(\ell_0)\left(\frac{\Delta x}{\ell_0}\right)^{\zeta}. \tag{4}$$

Note once again that for the same roughness exponent, the roughness measured over a given scale, ℓ_0, can be very small—and then the surface appears to be planar and the slopes are very small—or very large. The transition between these two situations occurs at the specific lateral scale, ℓ, defined so that the slope over the distance ℓ is unity, i.e. $\sigma(\ell) = \ell$. This length, known as the *topothesy*, directly gives an amplitude parameter and is of particular importance when dealing with fractal properties of the surface. Although widely used, the fractal dimension is not well defined for a self-affine surface. The obvious reason is that the fractal dimension characterizes primarily objects that are invariant under isotropic scale transformations (self-similar objects). In the case of self-affine surfaces one can easily show that a box counting argument [12] leads to different results for the fractal dimension, d_F, depending on whether the box size, ϵ, is smaller or larger than the topothesy, ℓ. In particular, it can be shown that the number of boxes of size ϵ, $\mathcal{N}(\epsilon)$, needed to cover a surface in d dimensions is

$$\mathcal{N}(\epsilon) \propto \begin{cases} \epsilon^{\zeta - d} & \epsilon < \ell \\ \epsilon^{1-d} & \epsilon > \ell. \end{cases} \tag{5a}$$

Hence, since $\mathcal{N}(\epsilon) \propto \epsilon^{-d_F}$ [12], it follows that the fractal dimension becomes

$$d_F = \begin{cases} d - \zeta & \epsilon < \ell \\ d - 1 & \epsilon > \ell \end{cases} \tag{5b}$$

and therefore in general depends on scale.

Although geometrically well defined, the topothesy is not always the most relevant amplitude parameter to use when dealing with a given physical problem. In the following we shall explore the scattering of an electromagnetic wave of wavelength λ from a rough self-affine metallic surface. We shall show that the scattering is directly controlled by the typical slope measured over one wavelength.

To summarize, self-affine surfaces are thus characterized by two parameters—the roughness or Hurst exponent, and an amplitude parameter. So far, however, we have said nothing about the range of validity of the self-affine scale invariance. Obviously, the range of validity of this invariance cannot be infinite in physical systems. We need to add two additional parameters—the lower and the upper cut-offs for the scale-invariant region, denoted by the length-scales ξ_- and ξ_+, respectively. Macroscopic roughness estimators are directly

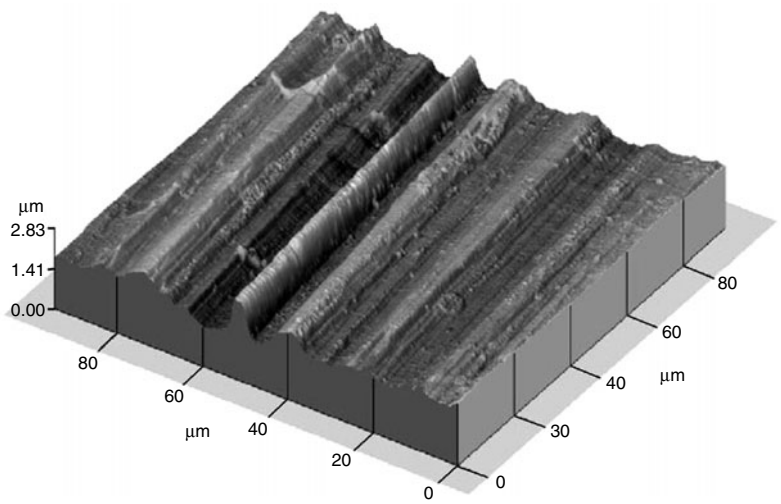

Figure 1. A 512 × 512 pixels AFM image of a cold-rolled aluminium alloy sheet. Notice the pronounced anisotropy of the surface due to the rolling process under which it was manufactured. The direction of the grooves is the rolling direction. After Plouraboué and Boehm [13].

controlled by these cut-offs. The global RMS roughness of the surface, σ, depends on the upper cut-off while the global RMS slope, s, depends on the lower cut-off according to

$$\sigma = \sigma(\xi_+) = \ell^{1-\zeta}\xi_+^{\zeta} \tag{6a}$$

and

$$s = s(\xi_-) = \ell^{1-\zeta}\xi_-^{\zeta-1}. \tag{6b}$$

In order to discuss scale invariance, one obviously requires that the scale separation between the cut-offs, $\xi_+ - \xi_-$, is large enough. However, the concept of scaling invariance does not need a huge range of validity in order to be useful. Height correlations measured on real surfaces are seldom perfectly Gaussian or exponential, but provided they are short range the approximation can be relevant. The same statement applies to self-affine surfaces. If the characteristic length of the physical system (the wavelength in the present case) lies within the range of validity of scale invariance; then the use of the concept of scale invariance can be justified. This remains relevant even if the range of validity is somewhat limited.

3. Electromagnetic wave scattering from self-affine surfaces

The angular distribution of the light scattered from rough surfaces has been studied for a long time [14, 15]. This distribution can be quantified through the experimentally accessible quantity known as the mean differential reflection coefficient (DRC), that we shall denote by $\langle \partial R_s/\partial\theta_s\rangle$. This quantity is defined as the fraction of the incident power that is scattered into an angular interval $\mathrm{d}\theta_s$ about the scattering angle θ_s [16, 17]. The DRC can be related to the scattering amplitude which describes the scattering process, and it can be separated into two terms: one term stemming from *coherent* or specular scattering, and another from *incoherent* or diffuse scattering. Of course, such a separation is not possible under experimental conditions, but is quite useful in theoretical studies. The integral of the mean DRC over all scattering angles is related to the total reflectance of the surface.

Previously [9, 10], we have studied the mean DRC for self-affine metallic surfaces. This has been done both by developing an approximative analytic expression and by numerical simulations. We derived a closed-form solution for the mean DRC in s polarization within the single-scattering Kirchhoff approximation [18]. The metal surface was approximated to be perfectly conducting. The central ingredient of this expression is the symmetric Lévy distribution [19], which contains the Gaussian distribution as a special case.

We have previously derived [9, 10] in detail the mean DRC in s polarization for a perfectly conducting self-affine surface characterized by roughness exponent ζ and topothesy ℓ as given by the following expression:

$$\left\langle \frac{\partial R_s}{\partial \theta_s} \right\rangle = \frac{s(\lambda)^{-\frac{1}{\zeta}} a^{-(\frac{1}{\zeta}-1)}}{\sqrt{2}\cos\theta_0} \frac{\cos\frac{\theta_s+\theta_0}{2}}{\cos^3\frac{\theta_s-\theta_0}{2}} \mathcal{L}_{2\zeta}\left(\frac{\sqrt{2}\tan\frac{\theta_s-\theta_0}{2}}{a^{\frac{1}{\zeta}-1} s(\lambda)^{\frac{1}{\zeta}}} \right) \tag{7a}$$

where

$$a = 2\pi\sqrt{2}\cos\frac{\theta_s+\theta_0}{2}\cos\frac{\theta_s-\theta_0}{2} \tag{7b}$$

and $s(\Delta x) = \sigma(\Delta x)/\Delta x$ is the mean (absolute) slope over a lateral distance, Δx, and is related (cf. equations (4) and (6*b*)) to the topothesy by

$$s(\Delta x) = \left(\frac{\ell}{\Delta x}\right)^{1-\zeta} \tag{7c}$$

and finally $\mathcal{L}_\alpha(x)$, with $0 < \alpha \leqslant 2$, denotes the centred symmetric Lévy distribution of order α and is defined as

$$\mathcal{L}_\alpha(x) = \frac{1}{2\pi}\int_{-\infty}^{\infty} \mathrm{d}k\, \mathrm{e}^{\mathrm{i}kx}\mathrm{e}^{-|k|^\alpha}. \tag{7d}$$

Here from the surface normal, the angle of incidence (θ_0) is measured positively in the anticlockwise direction and the scattering angle (θ_s) is measured positively in the clockwise direction.

The result, equations (7), is derived within the Kirchhoff approximation [15, 18]. This single-scattering approximation consists of replacing every point at the surface by the local

tangent plane. It allows us to use Fresnel formulae to obtain a local reflection coefficient. The existence of a finite lower cut-off for the scale-invariant regime ensures that one can define a tangent plane. It should also be stressed that in obtaining equations (7) one has implicitly assumed that the upper cut-off for the scaling region is infinite, with the consequence that one only obtains incoherent scattering.

As mentioned above, the width and the height of the incoherent peak are mainly controlled by the slope measure over the wavelength. Using a Taylor expansion of the Lévy function we obtain respectively for the height of the peak and its width at half maximum

$$\left\langle \frac{\partial R_s}{\partial \theta_s} \right\rangle \Big|_{\theta_s=\theta_0} \simeq \frac{\Gamma(\frac{1}{2\zeta})}{2\sqrt{2}\pi\zeta(2\sqrt{2}\pi\cos\theta_0)^{\frac{1}{\zeta}-1}s(\lambda)^{1/\zeta}} \tag{8}$$

and

$$w(\zeta, s(\lambda), \theta_0) \simeq 2\sqrt{\frac{\Gamma(\frac{1}{2\zeta})}{\Gamma(\frac{3}{2\zeta})}}(2\sqrt{2}\pi\cos\theta_0)^{\frac{1}{\zeta}-1}s(\lambda)^{1/\zeta} \tag{9}$$

where Γ corresponds to the gamma function. Note that although incoherent in nature, the peak can be extremely sharp for small values of the slope. Within the framework of this calculation we see that the scattering is mainly controlled by two parameters, the slope measure over the wavelength, $s(\lambda)$, and the roughness exponent ζ. In a equivalent way, the scattering from short-range correlated surfaces is controlled by the standard deviation of the roughness, and the correlation length [14, 15]. We saw above that these two additional parameters that bound the scale-invariant region are necessary to fully describe self-affine surfaces. What is the effect of these bounds on the scattering? The existence of a lower cut-off allows us to have a small-scale regularization of the surface and therefore justifies the use of the Kirchhoff approximation. Beyond this trivial assertion it appears that the lower cut-off does not play any role in the far-field scattering: all sub-wavelength details are smoothed out by the wave equation and the effective lower cut-off of the system is the wavelength. This assertion obviously does not apply to the near field. In this case, the surface fields are highly fluctuating and localized. Further, the amplitude of the fluctuations is directly controlled by the geometrical lower cut-off of the surface [8]. These fluctuations are, in fact, caused by sub-wavelength evanescent modes [8]. However, the upper cut-off, ξ_+, as we recall, did not enter explicitly into the above calculations and the results were actually obtained by assuming an infinite upper cut-off. However, as mentioned in [3], the effect of a finite upper cut-off is rather easy to handle. Provided $\xi_+ \gg \lambda$, we can consider that the incoherent part of the scattering remains unchanged while in addition a small coherent peak appears, whose amplitude is controlled by the global standard deviation of the surface roughness, which now, according to equation (6*a*), is finite, since ξ_+ is not infinite. In particular, the coherent contribution to the mean DRC depends directly on ξ_+ through the global RMS roughness, $\sigma = \ell^{1-\zeta}\xi_+^{\zeta}$ (cf. equation (6*a*)), and one can show that [15]

$$\left\langle \frac{\partial R_s}{\partial \theta_s} \right\rangle_{coh.} \propto \exp\left[-\left(\frac{2\pi}{\lambda}\sigma(\cos\theta_s + \cos\theta_0)\right)^2\right]. \tag{10}$$

For a plane incident wave the function of proportionality is the Dirac delta function $\delta(\theta_s - \theta_0)$, while for a finite-sized incident beam it is a smooth function decaying away from $\theta_s = \theta_0$. The amplitude of the coherent peak, given by equation (10), drops off very fast when the upper cut-off ξ_+ is increased due to the exponential function. The experimental measurements of these peaks have been intensively used in recent years to follow the development of roughness and spatial correlations for surfaces generated by deposition processes [4].

Recently, we compared the mean DRC in the Kirchhoff approximation with results obtained from rigorous numerical simulations [9, 10] and found agreement in the central angular region around $\theta_s = \theta_0$. However, the tails of the mean DRC obtained from the Kirchhoff approximation showed a systematic overestimation of the scattering as compared with the simulation results. This, we believe, corresponds to the failure of the Kirchhoff approximation to include shadowing and multiple-scattering effects which become non-negligible for grazing incidence and scattering. In the central region, the agreement between the Kirchhoff approximation and the numerical rigorous simulations is however striking (cf. section 4). As an illustration of the quality of this agreement we show here that we can even observe second-order effects predicted in the framework of the Kirchhoff approximation. It appears that the location of the incoherent peak is slightly shifted from the specular position for non-zero angles of incidence [10]. In this case the incoherent peak is located at $\theta_s = \theta_0 + \Delta\theta_0$, where $\Delta\theta_0$ ($\Delta\theta_0 \sim w^2 \ll w$) scales as

$$\begin{aligned}\Delta\theta_0 &\simeq -\frac{2\zeta-1}{\zeta}\frac{\Gamma(\frac{1}{2\zeta})}{\Gamma(\frac{3}{2\zeta})}\tan\theta_0(2\sqrt{2}\pi\cos\theta_0)^{\frac{2}{\zeta}-2}s(\lambda)^{2/\zeta} \\ &= -\frac{2\zeta-1}{4\zeta}\tan\theta_0 w^2(\zeta, s(\lambda), \theta_0)\end{aligned} \tag{11}$$

where the expression for the width, $w(\zeta, s(\lambda), \theta_0)$, has been given earlier by equation (9). This second-order effect can be obtained [10] through an expansion of the Lévy distribution around zero. As shown in figure 2, our numerical estimations for the angular shift are consistent with our predictions. The simulations were performed for rather rough aluminium surfaces and the locations of the peaks were simply estimated by a parabolic fit in the angular regions around the peaks.

Such simulations were performed by formulating the Maxwell equations as a coupled set of integral equations. This is achieved by taking advantage of Green's second integral identity in the plane as well as the boundary conditions satisfied by the fields and their normal derivatives on the self-affine surface. These integral equations can be converted into matrix equations and solved for the sources—the fields and their normal derivatives evaluated at the surface. From the knowledge of these sources, the scattered field at any point above the surface and therefore the mean DRC may be calculated. The whole detailed procedure for performing such Monte Carlo simulations can be found in [16, 17].

4. Application to the characterization of an industrial aluminium surface

Aluminium is a metal that is abundant in the earth's crust. However, it does not appear naturally in pure form, but instead has to be extracted from certain types of ore. It was therefore

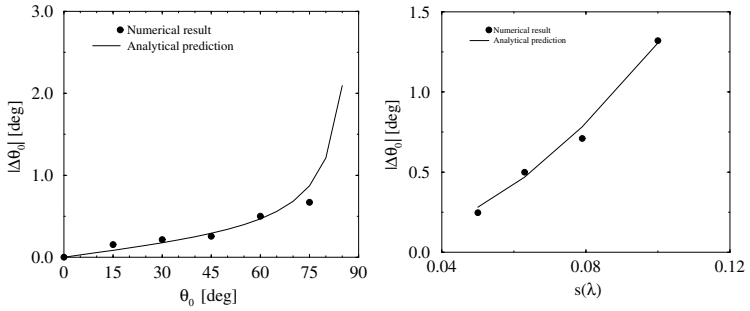

Figure 2. Shift of the incoherent peak of the mean DRC from the specular angular position versus angle of incidence for a slope of $s(\lambda) = 0.06$ (left) and versus the slope $s(\lambda)$ for an angle of incidence $\theta_0 = 60°$ (right). The wavelength of the incident light was $\lambda = 0.6328$ μm. We considered self-affine aluminium surfaces of roughness exponent $\zeta = 0.9$; the surface length was $L = 63.28$ μm $= 100\lambda$ discretized at $M = 512$ evenly distributed points. For the dielectric constant of aluminium at the wavelength of the incident light we used $\varepsilon(\omega) = -56.15 + i20.92$ [22]. The simulation results were obtained by averaging over $N = 5000$ surface realizations. The symbols correspond to results obtained from rigorous numerical simulations. The location of the incoherent peak was estimated by a parabolic fit in the specular region of the mean DRC. The solid curves correspond to the analytic predictions of the angular shifts obtained from the Kirchhoff approximation and given by equation (11).

of great industrial importance when Charles Martin Hall in the late 1880s invented a cheap process, based on electrolysis, for producing aluminium of high purity. Since then the use of aluminium has increased dramatically, partly because of its light weight, its conducting properties and ease of recycling, and today it finds its use in most parts of daily life—from the soda cans and aluminium foils in the kitchen to the bodies of aircrafts and some cars.

Aluminium plates are highly appreciated in many cooperative sectors. They are typically produced in rolling mills from huge aluminium bars that through rolling are gradually reduced to the desired thickness. The basic rolling process consists of two rotating steel cylinders with parallel main axes. They are separated by a distance—the roll-gap—of which the value is guided by the thickness of the plates one wants after that stage of the process. By forcing an aluminium plate of thickness larger than the roll-gap through the rotating rolls, the thickness of the plate is reduced. However, from mass conservation one easily realizes that the velocity of the incoming part of the plate must be smaller then that of the outgoing, and that these two velocities are both different from that of the rolls. Hence, it should be intuitively clear that plastic deformations as well as slipping between the steel rolls and the aluminium will take place in, or close to, the gap of the rolls. Thus, any dirt located in the rolling zone or roughness features of the surface of the rolls might result at the surface of the plates in elongated structures along the rolling direction. Such structures are known as rolling stripes, and are typical characteristics of rolled aluminium products.

In figure 1 we show an AFM image of the surface of an aluminium plate produced by (cold) rolling (after [13]). One immediately observes that this surface is far from being without any structure, and the rolling stripes are specially apparent. Recently it was shown that such surfaces show self-affine scaling behaviour [13] over a spatial region ranging from 50 nm up to 50 μm.

Instead of making AFM measurements, is it possible to instead use electromagnetic probes to characterize such metal surfaces? The advantages would be that optical techniques are inexpensive and versatile and that they can be incorporated into many different experimental set-ups [21]. They can also be used for *in situ* studies of surface growth without hampering the growth process itself as most probably the tip of an AFM would do. Furthermore, and even more important, optical techniques can cover large surface areas that can be many orders of magnitude larger than what can be probed by microscopy techniques in one single measurement. This is often crucial in order to guarantee that the surface area under study is representative of the whole macroscopic surface. However, to be able to extract surface information from electromagnetic scattering data, one has to be able to interpret such scattering data with confidence. Below, we shall give examples of how this can be done.

Scattering experiments from the surface topography depicted in figure 1 were recently performed by Vandembroucq *et al* [20]. Some of their results for the mean differential reflection coefficients $\langle \partial R_s / \partial \theta_s \rangle$ versus scattering angle θ_s are reproduced as open circles in figure 3 in log–linear (main figures) and linear–linear scales (insets). The wavelength of the s-polarized incident light was $\lambda = 0.6328$ μm, which corresponds to the wavelength of a He–Ne laser, and the angles of incidence used were $\theta_0 = 0°$ and $\theta_0 = 65°$ for the left-and right-hand panels of figure 3 respectively. It is crucial to realize for what follows that the scattered light was collected by a thin vertical slit, adjusted to integrate the scattering contributions corresponding to the direction *perpendicular* to the rolling direction. Such an experimental set-up makes the scattering geometry effectively one dimensional. Note also from figure 3 that the backscattering direction, $\theta_s = -\theta_0$, is hard to resolve experimentally due to the incident beam. It should be mentioned, since Vandembroucq *et al* used arbitrary units in their measurements, that they only measured the mean DRC up to a multiplicative constant. We have therefore used the freedom to adjust this constant to make the comparisons with simulation results more apparent.

The dashed curves in figure 3 represent the best fits of the mean DRC to the single-scattering Kirchhoff approximation, equations (7), to the experimental data. These fits correspond to the roughness parameter $\zeta = 0.78$ and a topothesy of $\ell = 2.79 \times 10^{-11}$ m $= 4.39 \times 10^{-5}\lambda$, and the wavelength of the incident light was the same as used in the experiments, $\lambda = 0.6328$ μm. From figure 3, we observe that the analytic expression, equations (7), rather accurately predicts the angular dependence of the mean DRC around the specular

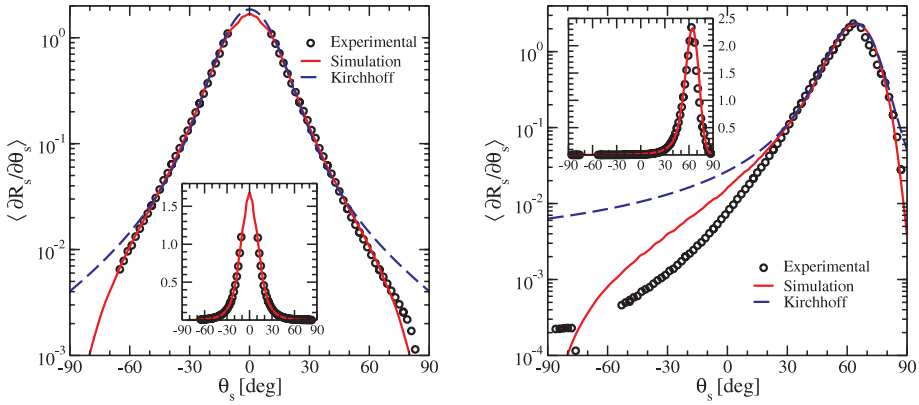

Figure 3. The mean differential reflection coefficient (DRC), $\langle \partial R_s/\partial\theta_s \rangle$, versus scattering angle, θ_s, for an aluminium self-affine surface of the type shown in figure 1 in log–linear (main panels) and linear–linear scale (insets). The incident light, of wavelength $\lambda = 0.6328\ \mu$m, was s polarized and was incident onto the cold-rolled aluminium surface at angles of incidence (left) $\theta_0 = 0°$ and (right) $\theta_0 = 65°$. The open circles represent the experimentally obtained scattering data obtained for the rough aluminium surface [20]. The solid curves are the results of rigorous numerical Monte Carlo simulations for the mean DRC of a self-affine aluminium surface of Hurst exponent $\zeta = 0.78$ and topothesy $\ell = 2.79 \times 10^{-11}$ m $= 4.39 \times 10^{-5}\lambda$. For the surface length we assumed $L = 63.28\ \mu\text{m} = 100\lambda$, that was discretized at $M = 1024$ evenly distributed points. For the dielectric constant of aluminium at the wavelength of the incident light we used $\varepsilon(\omega) = -56.15 + \text{i}20.92$ [22]. The simulation results were obtained by averaging over $N = 1500$ independent surface realizations. For the incident light we used a finite-sized beam of half width $g = 6.4\ \mu$m. The dashed curves are the prediction of equations (7) assuming the same roughness parameter and topothesy as for the surfaces used in the rigorous simulations. Note that since equations (7) assume a perfect conducting surface the normalization of the simulation results and the analytic approximation is a little different. Since the experimental data were obtained in arbitrary units, we have adjusted them by a constant amplitude to be able to compare with the simulation and analytic results.

(This figure is in colour only in the electronic version)

direction $\theta_s = \theta_0$, where the main scattered power is distributed. In particular, for normal incidence ($\theta_0 = 0°$), the analytic Kirchhoff result is accurate for scattering angles $|\theta_s| \leqslant 50°$. This region represents as much as 98.5% of the scattered energy, even though it overestimates the mean DRC for large scattering angles. The reason for these overestimations is most probably that multiple-scattering effects are not included. One should also recall that when using equations (7), the metallic self-affine surface is assumed to be a perfect conductor. This implies that the integral of the mean DRC over all scattering angles should be unity, i.e. all incident energy is scattered (and nothing absorbed). For the real aluminium surface, however, this quantity will be a little less than unity due to absorption.

In order to investigate multiple-scattering effects, we have performed rigorous computer simulations for the mean DRC of a self-affine surface characterized by the same parameters as above, i.e. by $\zeta = 0.78$ and $\ell = 4.39 \times 10^{-5}\lambda$. The Monte Carlo simulations were performed as described at the end of section 3. These results were obtained for a surface of length $L = 63.28\ \mu\text{m} = 100\lambda$ discretized over $M = 1024$ evenly distributed points. We used the dielectric constant of aluminium at the wavelength of the incident light $\varepsilon(\omega) = -56.15 + \text{i}20.92$ [22]. The results were averaged over $N = 1500$ independent realizations. Furthermore, to suppress edge effects, we used an incident finite-sized beam of half-width $g = 6.4\ \mu$m.

The solid curves in figure 3 represent the results for the mean DRC obtained from such rigorous computer simulations. We observe that the agreement with the experimental scattering results is rather good. In particular, for normal incidence the agreement is almost perfect for all scattering angles and over three orders of magnitude in intensity. The Monte Carlo result is in this case also able to catch the angular dependence of the mean DRC for the largest scattering angles where we earlier saw that the single-scattering Kirchhoff approximation failed by overestimating the mean DRC. This is an effect of including multiple-scattering effects in the analysis. Doing so will 'redistribute' into smaller scattering angles power that would according to a single-scattering theory have been reflected into large scattering angles (in absolute value). However, for non-normal incidence, here exemplified by the right-hand panel of figure 3 corresponding to an angle of incidence $\theta_0 = 65°$, the agreement between the experimental and Monte Carlo results becomes less good for angles $\theta_s < 30°$. At this point the intensity level has already dropped by 1.5 orders of magnitude compared with the value at the peak. For the scattering angles $\theta_s > 30°$ the agreement between the simulation results and the experimental data is good. This latter angular interval accounts for 97% of the scattered energy. The discrepancy between the simulation and experimental results for the mean DRC that can be observed in the right-hand panel of figure 3 we believe is caused by the scattering surface in fact being two dimensional and not one dimensional as assumed in order to generate the simulation results.

Since we also had access to AFM measurements of the topography of the surfaces used in the scattering experiments [13, 20], we can compare the self-affine surface parameters obtained *indirectly* from the experimental and simulation scattering results with those obtained *directly* from the measured surface topography. From the simulation results one recalls that we obtained a roughness exponent of $\zeta = 0.78$ and a topothesy of $\ell = 4.39 \times 10^{-5}\lambda$ with $\lambda = 0.6328\ \mu$m, or equivalently a slope over a wavelength (cf. equation (7*c*)) of $s(\lambda) = 0.11$. On the other hand, directly from the surface topography, measured by AFM in a direction perpendicular to the rolling direction, one obtains [20] $\zeta = 0.80 \pm 0.05$ and

$s(\lambda) = 0.11 \pm 0.01$. These results are therefore in excellent agreement with each other.

Hence, based on the obvious good agreement between the simulation and the single-scattering Kirchhoff results on the one hand, and the experimental scattering data on the other hand, we have demonstrated that electromagnetic scattering data can be used to characterize (industrial) self-affine metallic surfaces with confidence. Due to the extremely low computational cost of the analytic single-scattering Kirchhoff approximation result, equations (7), as compared with the rigorous numerical simulations, the analytic results presented here might be used for (almost) real-time *in situ* studies of self-affine surfaces. This may be of interest for example in sputtering and polishing experiments as well as for various surface deposition processes [12].

5. Conclusion

The scattering of s-polarized visible light from metallic self-affine surfaces has been studied. We showed that a Kirchhoff approximation reproduces nicely experimental and direct numerical simulation results for the scattering in the 'central angular region'. The quality of the agreement between the Kirchhoff approximation and numerical results is such that we could find evidence for a second-order effect: a slight shift of the incoherent peak from the specular direction in the case of finite angles of incidence. This is, to our knowledge, the first time that this effect has been numerically verified. Comparisons of experimental light scattering data collected from an aluminium sheet and rigorous numerical Monte Carlo simulation results proved to be extremely successful. For normal incidence such simulations predicted the experimental angular distribution of the scattered light for *all* scattering angles and over three orders of magnitude in intensity. The fact that we also obtained consistent results for grazing scattering angles shows that the discrepancies between the Kirchhoff approximation and the experimental results for these angles of incidence originate from the fact that multiple-scattering and shadowing effects were neglected in the Kirchhoff approximation and not from a failure of the self-affine description of the surface roughness. Based on the predictive power of the Kirchhoff approximation result and the Monte Carlo approach we showed that electromagnetic scattering can be used with great confidence in inverse scattering problems with the intention of characterizing self-affine surfaces. The surface parameters obtained from light scattering data were in perfect agreement with what could be obtained from direct surface topography measurements.

Acknowledgments

We wish to thank F Plouraboué, who initiated our interest in the scattering properties of cold-rolled aluminium surfaces. IS and DV wish to acknowledge the partial support of the French–Norwegian scientific cooperation programme AURORA for this work.

References

[1] Jakeman E 1986 *Fractals in Physics* ed L Pietronero and E Tossati (Amsterdam: Elsevier)
[2] Jordan D L, Hollins R C, Jakeman E and Prewett A 1988 *Surf. Topogr.* **1** 27
[3] Sinha S K, Sirota E B, Garoff S and Stanley H B 1988 *Phys. Rev.* B **38** 2297
[4] Zhao Y-P, Wang G-C and Lu T-M 2001 *Characterization of Amorphous and Crystalline Rough Surfaces—Principles and Applications* (Experimental Methods in the Physical Science 37) (New York: Academic)
[5] Sánchez-Gil J A and García-Ramos J V 1997 *Waves Random Media* **7** 285
[6] Sánchez-Gil J A and García-Ramos J V 1998 *J. Chem. Phys.* **108** 317
[7] Sánchez-Gil J A, García-Ramos J V and Méndez E R 2000 *Phys. Rev.* B **62** 10 515
[8] Sánchez-Gil J A, García-Ramos J V and Méndez E R 2001 *Opt. Lett.* **26** 1286
[9] Simonsen I, Vandembroucq D and Roux S 2000 *Phys. Rev.* E **61** 5914
[10] Simonsen I, Vandembroucq D and Roux S 2001 *J. Opt. Soc. Am.* A **18** 5914
[11] Bouchaud E 1997 *J. Phys.: Condens. Matter* **9** 4319
[12] Meakin P 1998 *Fractals, Scaling and Growth Far from Equilibrium* (Cambridge: Cambridge University Press)
[13] Plouraboué F and Boehm M 1999 *Trib. Int.* **32** 45
[14] Beckmann P and Spizzichino A 1963 *The Scattering from Electromagnetic Waves from Rough Surfaces* (Boston, MA: Artech)
[15] Ogilvy J A 1991 *Theory of Wave Scattering from Random Rough Surfaces* (Bristol: Institute of Physics)
[16] Maradudin A A, Michel T, McGurn A R and Méndez E R 1990 *Ann. Phys., NY* **203** 255
[17] Simonsen I 2000 *PhD Thesis* The Norwegian University of Science and Technology, Trondheim
[18] Born M and Wolf E 1999 *Principles of Optics* 7th edn (Cambridge: Cambridge University Press) (expanded)
[19] Lévy P 1937 *Théorie de l'Addition des Variables Aléatoires* (Paris: Gauthier-Villars)
[20] Vandembroucq D, Tarrats A, Greffet J-J, Roux S and Plouraboué F 2001 *Opt. Commun.* **187** 289
[21] Simonsen I, Lazzari R, Jupille J and Roux S 2000 *Phys. Rev.* B **61** 7722
[22] Palik E D 1985 *Handbook of Optical Constants of Solids* (New York: Academic)